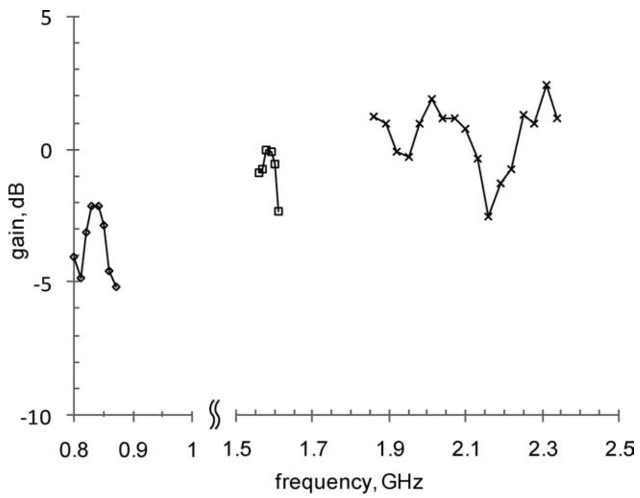

Figure 6 Antenna gains of proposed antenna

to perform multiresonance characteristics. The proposed antenna yields greater than -2.1 dBi of the antenna gain at GSM band and 2.45 dBi at WCDMA. This antenna is suitable for multiband antennas with narrowband selection characteristics for the services of multiple wireless communication systems of including GSM, GPS, DCS, PCS, and WCDMA bands.

ACKNOWLEDGMENTS

The present work was supported by the Special Research Grant of Sogang University, Korea and by the Korea Science and Engineering Foundation (KOSEF) grant funded by the Korea government (MEST) (No. 2010-0015919).

REFERENCES

1. Y. Jee and Y.-M. Seo, Triple-band CPW-fed compact monopole antennas for GSM/PCS/DCS/WCDMA applications, Electron Lett 45 (2009), 446–448.
2. B.H. Sun, J.F. Li, T. Zhou, and Q.Z. Liu, Planar meander sleeve monopole antenna for DVB-H/GSM mobile handsets, Electron Lett 44 (2008), 508–509.
3. S.C. Kim, S.H. Lee, and Y.-S. Kim, Multi-band monopole antenna using meander structure for handheld terminals, Electron Lett 44 (2008), 331–332.
4. X.-C. Lin and C.-C. Yu, A dual-band CPW-fed inductive slot-monopole hybrid antenna, IEEE Trans Antenn Propag 56 (2010), 282–285.
5. W.-C. Liu, Optimal design of dual-band CPW-fed G-shaped monopole antenna for WLAN application, Prog Electromagn Res 74 (2007), 21–38.
6. J.I. Kim and Y. Jee, Design of ultra-wideband coplanar waveguide-fed LI-shape planar monopole antennas, IEEE Antenn Wireless Propag Lett 6 (2007), 383–387.
7. A. Ghazi, M.N. Azarmanesh, and M. Ojaroudi, Multi-resonance square monopole antenna for ultra-wideband applications, Prog Electromagn Res C 14 (2010), 103–113.
8. R. Sujith, V. Deepu, D. Laila, C.K. Aanandan, K. Vasudevan, and P. Mohanan, A compact dual-band modified T-shaped CPW-fed monopole antenna, Microwave Opt Technol Lett 51 (2009), 937–939.
9. Z. Zhang, Y.C. Jiao, Y. Song, T.L. Zhang, S.M. Ning, and F.S. Zhang, A modified CPW-fed monopole antenna with very small ground for multiband WLAN applications, Microwave Opt Technol Lett 52 (2010), 463–466.

DIRECTION FINDING SYSTEM FOR AUTOMOTIVE APPLICATIONS USING SMALL PHASED ANTENNA ARRAY

Victor Rabinovich
Victenna Design and Consulting, 7 Moonlight Lane Richmond Hill, Ontario, Canada; Corresponding author: vrabinov@gmail.com

Received 11 January 2011

ABSTRACT: *Direction finding technique for car location in large parking lots is presented. Method uses compact phased antenna array with two-bit phase shifters. Proposed array operates as an intermediary between a car owner hand-held unit and car electronic circuit with small omnidirectional antenna. Only one antenna array for all cars is that utilized for car finding service. Experimental results confirm math estimations and MATLAB simulation.* © 2011 Wiley Periodicals, Inc. Microwave Opt Technol Lett 53:2441–2446, 2011; View this article online at wileyonlinelibrary.com. DOI 10.1002/mop.26275

Key words: *car finding; compacted phased antenna array; digital phase shifters; short range communication*

1. INTRODUCTION

Radio direction finding (DF) is a method that detects the arrival angle or the coordinates of incoming radio signals. DF systems have a wide range of applications, for example, they are used to track launches of rockets and their resulting trajectories, include emergency services, and HAM radios. Our article describes the car finding system in large parking lots, however is not limited by automotive applications.

The difficulty to find a car in a large parking lot or multilevel parking structures, at shopping or airport centers, close to the music or sporting events can be very annoying. The problem is so common that many parking ramps have special cars to drive people around to help them finding their car. A number of radio DF techniques [1–8] and devices become available offering a solution to this common daily problem.

For example, global positioning system (GPS) system [1] can be used in the open parking area. However, GPS signal strength is not enough to locate the vehicle in closed parking lots. Cost is another issue because such technique requires GPS equipment in each car that uses DF service.

According to the logic of the simplest DF system with omnidirectional vehicle mounted antenna [2] car owner presses a button of the hand-held transmitting module, and a receiver mounted on the vehicle turns on flushing light or horn sound which can be recognized by the motorist. However, the area in big parking lot includes a lot of sections and car owner can miss a response from the light or sound signal.

More sophisticated and advanced DF systems have an antenna array mounted on each vehicle that provides this service [3–6]. The antenna array elements can be combined using different schematics. One implementation uses one receiver channel per one antenna array element [3, 5]. Some of the DF systems use a single receiver with multiple array elements [6, 7] along with some form of switching among the elements.

Beam steering phased antenna array [8] with electronically controlled phase shifters can be used for DF applications. Most of phase shifters in use are digital. It is known [9] that accuracy of the angle-of-arrival (AOA) estimation increases for large antenna array with multibit digital phase shifters. Typically complicate and expensive multielement arrays are employed for military applications.

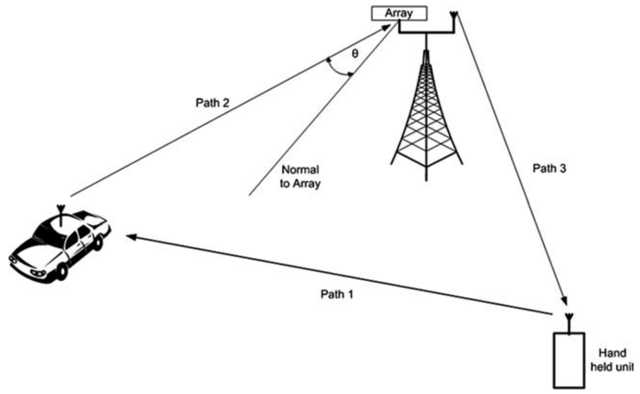

Figure 1 Communication scenario with receiving antenna array mounted on the lighting pole

Our article describes DF system that includes low cost compact electronically controlled phased antenna array with two-bit phase shifters. We propose specific phase variations of phase shifters and processing algorithm that improves resolution of AOA estimation. Additionally, suggested design requires the installation of only one receiving directional antenna array mounted on the ground beacon or lighting pole in the parking lot area.

2. COMMUNICATION SCENARIO

Figure 1 shows proposed communication scenario. Radio frequency (RF) signal radiated by an antenna of the hand-held car owner transmitter/receiver unit (path 1 shown in Fig. 1) is received by a compact omnidirectional antenna mounted on the car. For example, it can use omnidirectional antenna mounted on the car roof [10] with communication range of about two hundred meters. However, using omnidirectional antenna design does not allow estimation of car angle coordinates with respect to a reference orientation, for example, magnetic north. Therefore, proposed communication system uses more sophisticated antenna array system installed on special beacon or on the lighting pole in the parking area. Accurate angle position of the incoming RF source can be estimated with planar array or two linear perpendicular arrays [8]. Therefore, we will demonstrate the basic principle of the new technique on the example of linear antenna array.

As it is shown in Figure 1 car omnidirectional antenna retransmits the signal received from the hand-held unit (path 2) with identification code that belongs to the owner vehicle. Retransmitted signal is received by the antenna array system. Antenna array processor activated only for the signals with car identification code calculates AOA of the vehicle with respect to the reference angle position, omnidirectional base station antenna transmits signal with AOA data (path 3 in Fig. 1) and driver's hand-held unit records this information. According to this information car owner moves towards the car location. Direction information can be updated as car owner moves relative to the car.

It is very important that described communication logic excludes the mounting of an array on each vehicle and therefore simplifies the cost of the DF system.

3. ANTENNA ARRAY SYSTEM

Antenna array is the key of the DF system. Our target here is to design small phased antenna array with simple two-bit digital phase shifters [11] and a processor procedure which estimates bearing angle information from the received by an antenna array signal using only power measurements. Design is based on holography principle [12], and block diagram of investigated antenna is shown in Figure 2. Linear antenna array consists of N equally half wave spaced elements (below we use four elements as the base design for experiments). Each of N-1 antenna elements with uniform amplitude distribution has electronically controlled two-bit digit phase shifters, for example, based on pin-diode switchers [11]. Two-bit phase shifter changes phase of the signal captured by the antenna element in the range 0–360° with a discrete equal 90°. One reference channel without a phase shifter has a low noise amplifier with gain G. Antenna array has simple summing feed network based, for example, on a microstrip printed parallel combiner. Output of combiner is connected with a power estimator; the output of power estimator is connected with a digital correlator; and the output of digital correlator is connected with a beamforming processor that estimates the AOA.

It is known that regular scanning phased array with two-bit digital phase shifters can significantly degrade beam pointing performance [9]. Consider, for example, array with three omnidirectional elements (adjacent element distance is equal to half of the wavelength). Table 1 presents calculated two-bit phase values φ_n (in degrees) for each antenna element for scanning angle θ_0 in the range from 10 to 80°.

As we see from the table, for scanning angles θ_0 from 10 to 20° or from 50 to 60°, or from 70 to 80° two-bit phase shifters realize the same phase code combination. It means that such phased array configuration does not provide accurate beam direction pointing.

Idea of proposed here solution consists of phase manipulation (using two-bit phase shifter) of the signal captured by each array element, recording of power variations received at the array output, processing of these variations with digital correlator and beamforming processing that estimates AOA of incoming signal.

4. DESCRIPTION OF PROCESSING ALGORITHM

Proposed procedure includes measuring an antenna array power variations $P_k(\theta,r)$ (using power estimator shown in Fig. 2) caused by phase changes $\Delta\varphi_r = \pi r/2$ of the k-th element's phase shifter (k = 1, 2, N-1). Position of the incoming source is determined by AOA θ.

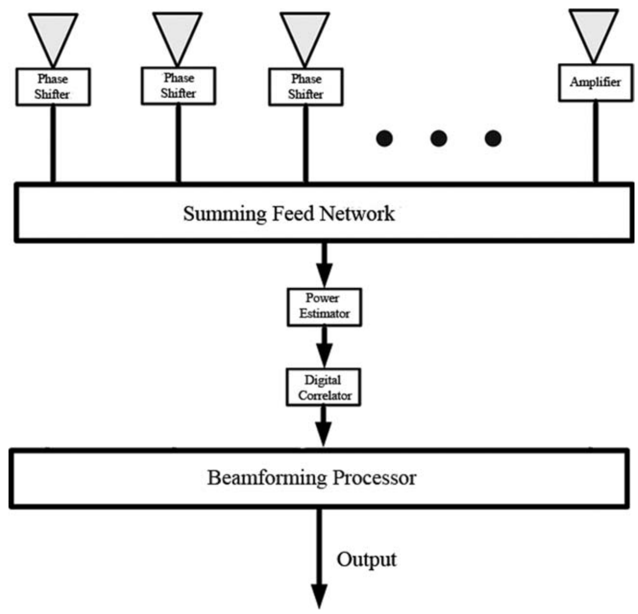

Figure 2 Phased antenna array system block diagram

TABLE 1 Phase Shifts for Regular Three Elements Electrically Beam Scanning Array with Two-Bit Phase Shifters within Scanning Angle Range From 10 to 80°

θ_0	φ_1	φ_2	φ_3
10	0	90	90
20	0	90	90
30	0	90	180
40	0	90	270
50	0	180	270
60	0	180	270
70	0	180	0
80	0	180	0

Measured results are processed with digital correlator

$$\mathrm{Re}_k(\theta) = \sum_{r=1}^{4} P_k(\theta, r) \cdot \cos(\pi \cdot r/2) \tag{1}$$

$$Jm_k(\theta) = \sum_{r=1}^{4} P_k(\theta, r) \cdot \sin(\pi \cdot r/2) \tag{2}$$

Values in Eqs. (1) and (2) can be expressed in complex form

$$E_k(\theta) = \mathrm{Re}_k(\theta) + j \cdot Jm_\mathrm{k}(\theta) \tag{3}$$

or

$$E_k(\theta) = |E_k(\theta)| \cdot e^{j \cdot \psi_k(\theta)}$$

Calculated values in Eq. (3) are multiplied with complex weights w_k (θ_0) = $e^{j\pi \cdot (k-1) \cdot \sin\theta_0}$ in beamforming processor, and function $F(\theta,\theta_0)$ is estimated for different scanning angles θ_0

$$F(\theta, \theta_0) = \sum_{k=1}^{N-1} E_k(\theta) \cdot e^{j\pi \cdot (k-1) \cdot \sin\theta_0} \tag{4}$$

We will show that if an amplifier gain G of the reference channel is more than the number of the antenna array elements, then expression in Eq. (4) determines the AOA of the RF incoming signal.

5. ANALYSIS OF AOA ALGORITHM

Power of the signal received by a linear phased antenna array (up to a constant factor independent on the element number) due to phase change at k-th element in interval 0–360° with a discrete 90° can be expressed as

$$P_k(\theta_0, r) = |B_k(\theta) \cdot e^{j\phi_k} + D_k(\theta) \cdot e^{j(\pi(k-1) \cdot \sin\theta + \pi \cdot r/2)} + G \cdot D_N(\theta) \cdot e^{j(\pi \cdot (N-1) \cdot \sin\theta + \varepsilon)}|^2 \tag{5}$$

Array with equally half wave spaced elements and uniform amplitude distribution consists of (N-1) elements with phase shifters and one reference element with low noise amplifier; k = 1, 2, 3, … N-1.

$D_k(\theta)$ = radiation pattern of the k-th element toward the arrival angle direction θ.

Reference element of the array is connected to a summing network via the low noise amplifier with a gain equal $G \cdot e^{j\varepsilon}$.

$$B_k(\theta) \cdot e^{j\phi_k} = \sum_{n=1}^{N-1} D_n(\theta) \cdot e^{j \cdot \pi \cdot (n-1) \cdot \sin\theta} - D_k(\theta) \cdot e^{j \cdot \pi \cdot (k-1) \cdot \sin\theta} \tag{6}$$

Measured data in Eq. (5) can be expressed as following:

$$P_k(\theta, r) = S_{k0}(\theta) + S_{k1}(\theta, r) + S_{k2}(\theta, r) \tag{7}$$

where

$$S_{k0}(\theta) = B_k^2(\theta) + D_k^2(\theta) + (G \cdot D_N(\theta))^2 + 2B_k(\theta) \cdot G \cdot D_N(\theta) \cdot \cos(\delta_k) \tag{8}$$

$$\delta_k = \pi \cdot (N-1) \cdot \sin\theta + \varepsilon - \phi_k$$

$$S_{k1}(\theta, r) = 2B_k(\theta) \cdot D_k(\theta) \cdot \cos(\pi \cdot (k-1) \cdot \sin\theta + \pi \cdot r/2 - \phi_k) \tag{9}$$

$$S_{k2}(\theta, r) = 2G \cdot D_N(\theta) \cdot D_k(\theta) \cdot \cos(\pi \cdot (k-N) \cdot \sin\theta + \pi \cdot r/2 - \varepsilon) \tag{10}$$

For simplification, assume that radiation patterns of the different antenna elements $D_k(\theta)$ are identical, i.e. $D_k(\theta) = D(\theta)$; k = 1, 2, 3, … N.

Substituting Eqs. (7), (8), (9), and (10) into Eqs. (1) and (2) the result can be written as

$$E_k(\theta) = 4 \cdot D^2(\theta) \cdot e^{-j \cdot \pi \cdot (k-1) \cdot \sin\theta} \cdot \left(C_k(\theta) \cdot e^{j\phi_k} + e^{j \cdot (\pi \cdot (N-1) \cdot \sin\theta + \varepsilon)}\right) \tag{11}$$

where $C_k(\theta) \cdot e^{j\phi_k} = F_0(\theta) - e^{j \cdot \pi \cdot (k-1) \cdot \sin\theta}$, and $F_0(\theta) = \sum_{k=1}^{N-1} e^{j \cdot \pi \cdot (k-1) \cdot \sin\theta}$.

Beamforming processor computes formula (4) based on the expression (11)

$$F(\theta, \theta_0) = \sum_{k=1}^{N-1} E_k(\theta) \cdot e^{-j\pi \cdot (k-1) \cdot \sin\theta_0} = F_1(\theta, \theta_0) + F_2(\theta, \theta_0) \tag{12}$$

where

$$F_1(\theta, \theta_0) = 4 \cdot D^2(\theta) \cdot \sum_{k=1}^{N-1} C_k(\theta) \cdot e^{j\phi_k} \cdot e^{j \cdot \pi \cdot (k-1) \cdot (\sin\theta_0 - \sin\theta)} \tag{13}$$

$$F_2(\theta, \theta_0) = 4G \cdot D^2(\theta) \cdot e^{j \cdot (\pi \cdot (N-1) \cdot \sin\theta + \varepsilon)} \cdot \sum_{k=1}^{N-1} e^{j \cdot \pi \cdot (k-1) \cdot (\sin\theta_0 - \sin\theta)} \tag{14}$$

Output of beamforming processor has two components: component (14) with a maximum absolute value equal $q_2 = 4G \cdot (N - 1) \cdot D^2(\theta)$ directed to the scanning angle θ_0 equal arrival angle θ and component (13) with absolute maximum value $q_1 = 4 \cdot D^2(\theta) \cdot |F_0(\theta)| \cdot (N-2)$ for $\theta_0 = \theta$. If the ratio q_2/q_1 is much larger than 1, then expression (12) determined by (14) estimates AOA. Because maximum value of $|F_0(\theta)|$ is equal $|F_{0\max}(\theta = 0)| = (N-1)$ condition $q_2/q_1 \gg 1$ corresponds to the expression

$$G >> (N-2) \tag{15}$$

Ratio (15) means that amplifier gain G has to be much larger than the number of the elements. Correct AOA estimation as a function of the amplifier gain will be based on the simulation results of the proposed process.

6. SIMULATION RESULTS

MATLAB software simulations are conducted for equally spaced N omnidirectional antenna array system shown in Figure 2 with uniform amplitude distribution and the distance between

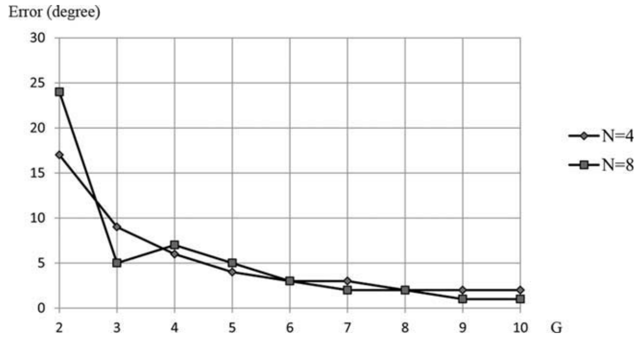

Figure 3 Angle error for different amplifier gain values

elements equal half of the free space wave. Figure 3 presents the maximum absolute angle error in beam pointing as a function of the amplifier gain G. Each angle error is calculated as a maximum value within the arrival angle range θ of 5–80°. It is seen that for the gain values 12 dB in Eq. (4) and more angle error does not exceed 7° for both four and eight element antenna arrays. It means that acceptable AOA error can be reached for the amplifier gain value less than is determined by the ratio (15).

In practice, digital phase shifters exhibit discrete phase shifts $\pi \cdot r/2$ with errors $\xi_k(r)$, i.e. $\eta_k(r) = \pi \cdot r/2 + \xi_k(r)$ ($r = 0,1,2,3$), where k = element number, r = number of phase discrete. Typically phase errors $\xi_k(r)$ vary randomly from one phase state to the other and from one number of element to the other. As a result, these errors cause additional antenna array errors in beam pointing, gain reductions, increasing of average sidelobe level, perhaps shape change. For us the most important parameter is the beam pointing value. Figures 4a and 4b and 5a and 5b show simulation

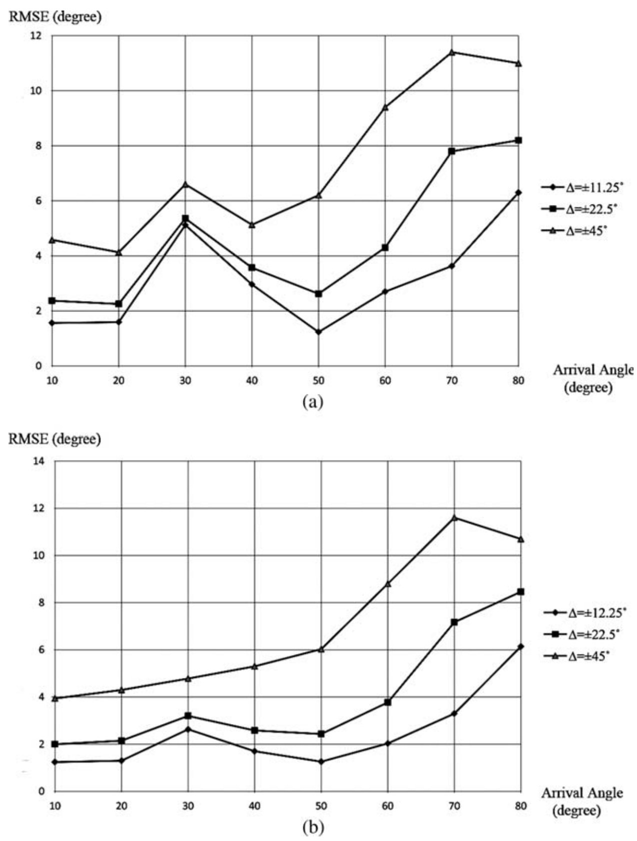

Figure 4 (a) RMSE as a function of the original AOA, $N = 4$, $G = 15$ dB, simulation results. (b) RMSE as a function of the original AOA, $N = 4$, $G = 20$ dB, simulation results

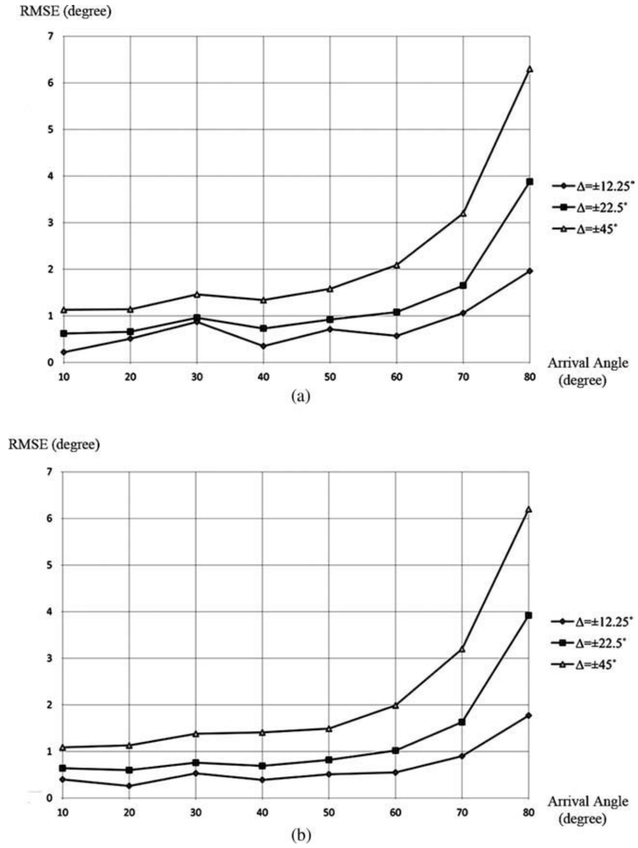

Figure 5 (a) RMSE as a function of the original AOA, $N = 8$, $G = 15$ dB, simulation results. (b) RMSE as a function of the original AOA, $N = 8$, $G = 20$ dB, simulation results

results of the root mean square error (RMSE) in beam pointing value (in degrees) as a function of the original RF source angle location. RMSE results based on 500 random phase error sets $\xi_k^m(r)$ are drawn as a function of the arrival angle θ (m = set number; n = array element number; $r = 0, 1, 2, 3$). Each phase error set values $\xi_n(r)$ are assumed to be uniformly distributed random in the following intervals: $\Delta = \pm 11.25°$ or $\Delta = \pm\ 22.5^0$, or $\Delta = \pm 45°$ independent for different r and n numbers. Error $\varepsilon_m = \theta_{\text{est}}^m - \theta$ ($m = 1, 2, \ldots, 500$; θ_{est}^m = estimated arrival angle) is calculated for each m number and then $RMSE = \sqrt{\sum_{m=1}^{500} \varepsilon_m^2 / 500}$ is estimated. Results are presented for four and eight array elements. Simulation presented in Figures 4 and 5 shows that RMSE values calculated for two different amplifier gains equal 15 and 20 dB are almost the same.

Multipath fading is another source of the error estimation in beam pointing angle. Because of the varying path lengths, phases, amplitudes, and angles of arrival for the reflected waves are random, the received by each array element reflected signal becomes a random variable. Signal impinging on n-th element of the equally half of the wave length spaced antenna array with uniform amplitude distribution and identical radiation patterns of antenna elements can be expressed as

$$S(n) = \alpha_0 \cdot D(\theta) \cdot e^{j \cdot (\pi \cdot (n-1) \cdot \sin\theta + \varphi)} + D(\theta) \cdot \sum_{m=1}^{M} \alpha_m \cdot e^{i(\pi \cdot (n-1) \cdot \sin\theta_m + \gamma_m)} \qquad (16)$$

First component of the expression (16) is line-of-sight signal and second parasitic component includes a number of waves reflected

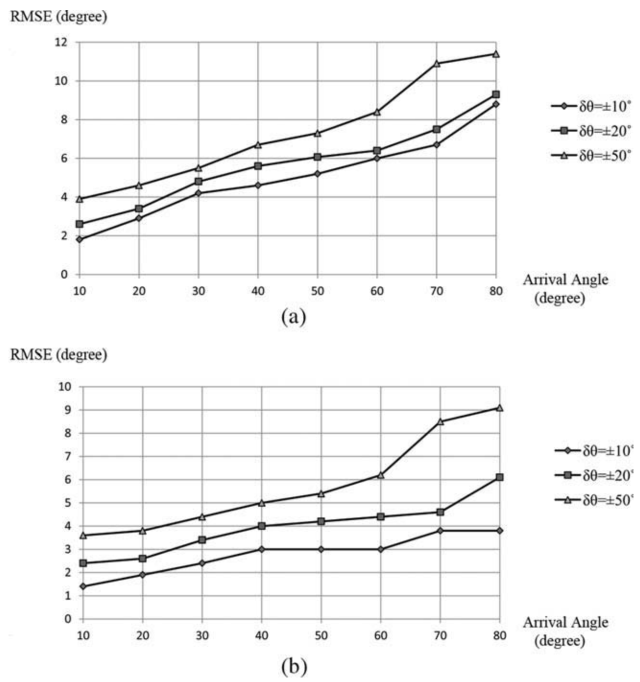

Figure 6 (a) RMSE for multipath fading as a function of the original AOA, $N = 4$, $G = 15$ dB, signal/noise ratio = 10 dB, simulation results. (b) RMSE for multipath fading as a function of the original AOA, $N = 4$, $G = 20$ dB, signal/noise ratio = 10 dB, simulation results

and scattered by cars that surround driver's car. For computer simulation we consider Jakes modeling method of scatters modeling [13]:

a. Signals received by an antenna array are assumed to be plane waves;
b. Random and independent for different scattering waves amplitudes α_m of scatters have Rayleigh distribution;

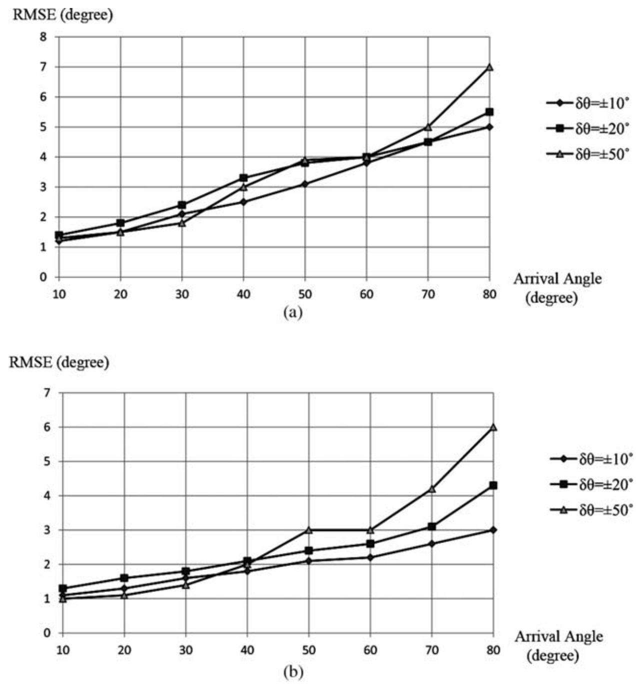

Figure 7 (a) RMSE for multipath fading as a function of the original AOA, $N = 8$, $G = 15$ dB, signal/noise ratio = 10 dB, simulation results. (b) RMSE for multipath fading as a function of the original AOA, $N = 8$, $G = 20$ dB, signal/noise ratio = 10 dB, simulation results

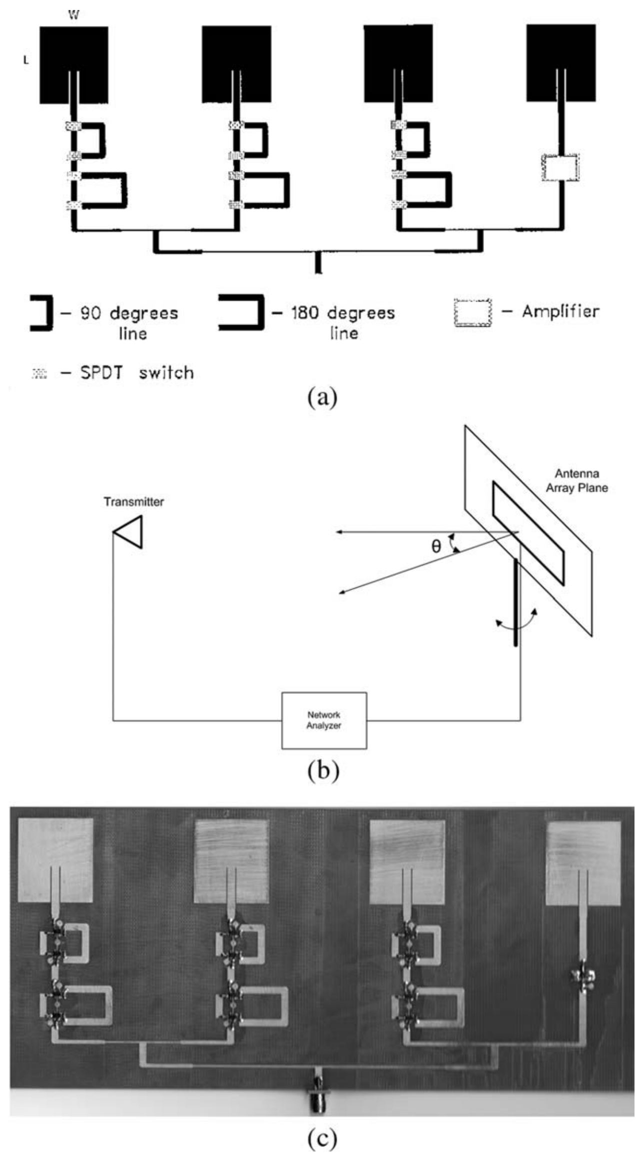

Figure 8 (a) Block diagram of four elements antenna array with three two-bit phase shifters and one reference channel with an amplifier. (b) Direction finder measurement setup with an antenna array. (c) Photograph of the fabricated array prototype

c. Random phases γ_m are uniformly distributed over interval $[-\pi\ \pi]$ for all k and they are mutually independent;
d. Angle of arrival θ_m is a random value uniformly distributed over the interval $\theta \pm \delta\theta$. Note, that θ is an angle of RF source arrival (amplitude of this signal is α_0). We used $M = 50$ harmonics for simulation process.

Figures 6 and 7 show simulation results of the RMSE based on 500 random samplings for the signal to noise ratio 10 dB ($\sum_{m=1}^{M} \alpha_m^2/\alpha_0^2 = 10$). Calculated for four and eight elements array and for amplifier gain values 15 and 20 dB curves as a function of arrival angle θ are presented for different $\delta\theta$ values: $\pm10°$, $\pm20°$, and $\pm50°$.

7. EXPERIMENTAL RESULTS

Experimental AOA measurements were conducted with four elements array that includes three elements with two-bit phase shifters and one element with low noise amplifier. Block diagram of the array is shown in Figure8a. Each element operating at 2 GHz presents linear polarized patch antenna with the following

TABLE 2 Power Estimator Measurements Due to Phase Variations at the Array Elements, Angle of Arrival $\theta = 20°$

$k \backslash r$	$r = 0$	$r = 1$	$r = 2$	$r = 3$
$k = 1$	0	−0.2	2.29	1.58
$k = 2$	0	−1.6	0.31	1.39
$k = 3$	0	−2.76	−4.98	−0.42

dimensions: length $L = 35.9$ mm, width $W = 32$ mm. Inserted microstrip feed line section provides 50 Ω input element impedance. Two-bit phase shifters are implemented on the base of switched-line concept, which uses electronically controlled switches and lines of different lengths to obtain a set of phase steps. Outputs of the antenna array elements are connected with 50 Ω inputs of feed line that has 50 Ω output impedance and combines all signals into one output. AOA measurement setup is shown in Figure 8b. Linear array mounted on turn table can change azimuth position relative to RF incoming source angle.

Photograph of the fabricated array prototype is shown in Figure 8c. Designed array is fabricated on an $h = 1.6$ mm FR-4 substrate with an element separation equal 7.5 cm which is 0.5 of the free space wave length. Switch system consists of commercially available SPDT switches RF2436 from RF Micro Devices. Array is built according to the block diagram shown in Figure 8a. Integrated amplifier ERA-6 (measured gain is about 9 dB) is used for amplification in reference channel. Power supplier and control circuits are placed on the back side of the FR-4 board.

Two series of experiments were conducted with four antenna array elements: first one refers to the RF wave coming from the angle $\theta = 20°$ to the array normal and the other one- to $\theta = 40°$. Tables 2 and 3 show power measurements results P_k (θ, r) (dB scale normalized to the value P_k $(\theta, 0)$) due to the differential phase shifts 0° ($r = 0$), 90° ($r = 1$), 180° ($r = 2$), and 270° ($r = 3$) realized by k-th element phase shifter.

Using power measurement results and formulas (1)–(4) we estimated arrival angle θ_{est}: $\theta_{est}(\theta = 20°) = 22°$ and $\theta_{est}(\theta = 40°) = 34°$. Simulations based on an amplifier gain equal 10 dB in reference channel show $\theta_{est0}(\theta = 20°) = 21°$ and $\theta_{est0}(\theta = 40°) = 36°$. We see good agreement between measurements and simulation. The error 4° between simulation and original AOA for original arrival angle equal 40° can be reduced up to 1° by increasing the amplifier gain to the value 20 dB.

Table 4 demonstrates the effect of instrumental errors in power measurements. We used power measurement data from Table 3, added random errors (imitating measurement errors) and performed AOA algorithm. Table 4 shows 10 AOA estimations for uniformly randomly distributed instrumental errors: column 1 corresponds to the interval ±0.5 dB; column 2 -to the interval ±1 dB; and column 3- to the interval ±2 dB.

It is seen that random errors in power measurements ±2 dB or less do not effect on AOA errors more than 10°.

8. CONCLUSION

We investigate car angle position system proposed for automotive applications particular for determination of the car location in large parking lot. Key of the system is small phased antenna array. Array consists of small number of elements with two-bit phase shifters and one reference element with an amplifier. Computer modeling is presented for four and eight array elements. Simulation results are shown as functions of the algorithm processing errors, phase shifters errors, and multipath fading errors. Amplifier gain value that provides minimal angle error for AOA estimation is defined. Experimental results for the array with four elements confirm the efficiency of proposed algorithm.

TABLE 3 Power Estimator Measurements Due to Phase Variations at the Array Elements, Angle of Arrival $\theta = 40°$

$k \backslash r$	$r = 0$	$r = 1$	$r = 2$	$r = 3$
$k = 1$	0	−1.5	−3.8	−3.6
$k = 2$	0	3.3	4.5	0.3
$k = 3$	0	−4	0	−3.1

TABLE 4 AOA Estimation for Random Errors in Power Estimator Measurements

±0.5 dB	35°	36°	38°	35°	37°	38°	38°	35°	36°	38°
±1 dB	35°	34°	36°	34°	39°	34°	35°	34°	37°	37°
±2 dB	33°	30°	34°	26°	42°	44°	45°	35°	34°	38°

REFERENCES

1. R. Christ, Application and Performance of Personnel Tracking Systems, Security Technology, In: 43rd annual 2009 international Carnahan conference on, 120–128.
2. J.H. Bullock, Vehicle locator system, US Patent, 5768758, 1998.
3. D.N. Aloi and M.S. Sharawi, Comparative analysis of single-channel direction finding algorithms for automotive applications at 2400 MHz in a complex reflecting environment, Phys Commun 3 (2010), 19–27.
4. A. Tieman et al., ‘‘Vehicle locator key fob with range and bearing measurement’’, US Patent Application Publication, 2009/0264082, 2009.
5. V. Vu and A. Delai, Digital solution for inter-vehicle localization system by means of direction-of-arrival, In: International symposium on intelligent signal processing and communication systems (ISPACS2006), 875–878.
6. R. Bruzzone, Radio signal direction finding, US Patent 6,271,791, 2001.
7. D. Peavey and T. Ogunfunmi, The single channel interferometer using a pseudo-doppler direction finding system, In: Proceeding of 1997 conference on acoustic, speech, and signal processing, 5 (1997), 4129–4132.
8. R.C. Hansen, Phased array antennas, 2nd ed., Wiley, New York, NY, 2009.
9. B.R. Hatcher, Granularity of beam positions in digital phased arrays, Proc IEEE, 56 (1968), 1795–1800
10. V. Rabinovich and D. Rabinovich, Three port compact multifunction printed antenna system, antenna for automotive applications, IEEE Antennas Propag Soc Int Symp, Toronto, Canada (2010).
11. Leo G. Maloratsky, Electrically tunable switched-line diode phase shifters. High frequency electronics, 2010.
12. G. Deschamps, Some remarks on radio frequency holography, Proc IEEE, 55 (1967), 570–571.
13. W.C.Y. Lee, Mobile communications engineering, 2nd ed., McGraw Hill, New York, NY, 1998.

BANDWIDTH ENHANCEMENT OF MICROSTRIP ANTENNAS BY STAGGERING EFFECT

K. Mandal,[1] S. Sarkar,[2] and P. P. Sarkar[2]
[1] Academy of Technology, Hooghly, (W.B.), India
[2] DETS, University of Kalyani, Kalyani, (W.B.), India;
Corresponding author: parthabe91@yahoo.co.in

Received 29 December 2011

ABSTRACT: *A structure of staggered tuned microstrip antenna is designed and fabricated. Theoretical and experimental investigations are done on the structure. Both the results show that due to staggering*